the Soneira-Peebles Model

Rien van de Weygaert & Willem Schaap

Kapteyn Astronomical Institute, University of Groningen

Lecture Course
"Large Scale Structure in the Universe"
Febr-April 2007

1 the Soneira-Peebles model

In the late seventies Soneira & Peebles (1977) (also see Soneira & Peebles 1978) noticed that the observed angular galaxy distribution on the sky displays self-similar behavior. They succeeded in reproducing the main clustering statistics of this distribution with a simple analytic model with only a few adjustable parameters, which determine the complexity and dynamic range of the resulting point distribution. Because these properties may be varied in a predictable fashion, we have used the Soneira-Peebles model to test the performance of the DTFE with respect to point distributions with a similar dynamic range as the observed galaxy distribution on the sky.

In essence, the Soneira-Peebles model consists of a recipe to distribute a given number of points. The starting point is a level-0 sphere of radius R. In this sphere η level-1 spheres are placed with radius R/λ and $\lambda > 1$. The new spheres are placed at a random position inside the level-0 circle, such that their centers fall inside the original level-0 sphere. Within each of these η level-1 spheres, one places η level-2 spheres of radius R/λ^2. This process is repeated until one ends up with in total η^L level-L spheres of radius R/λ^L. At the center of each of these level-L spheres a point is placed. One therefore ends up with in total η^L points, which in the Soneira-Peebles model represent galaxies. We will refer to this procedure up to this point as the *singular Soneira-Peebles model*. This procedure is illustrated in the top panel of Fig. 1.

The Soneira-Peebles model is controlled through three parameters, η, L and λ. The effect of varying these parameters on the resulting point distribution is illustrated in the 2nd to 4th row of Fig. 1. For a given number of points, η determines the dynamic range of the resulting point distribution. For a small value of η, many levels are needed to reach a fixed number of points, while a large value of η results in a smaller number of levels. A small value of η also results in a smaller filling fraction of space with spheres than a high value of η (2nd row in Fig. 1). L denotes the total number of levels and therefore determines the range of densities and scales in the resulting point distribution. For a fixed value of η, L also determines the total number of points (third row in Fig. 1). Finally, for given values of η and L, λ determines the range of spatial scales. A value of λ close to 1 means that subsequent spheres of higher levels are of comparable size. Values of λ much larger than one mean that each subsequent level consists of spheres which are significantly smaller than the spheres in the preceding level (bottom row in Fig. 1).

An important property of the Soneira-Peebles model is that it is one of the few analytic self-similar models of the galaxy distribution for which the two-point correlation function can be analytically evaluated. In M dimensions it is given by

$$\xi(r) \sim r^{-\gamma} , \tag{1}$$

with

$$\gamma = M - \left(\frac{\log \eta}{\log \lambda} \right) \quad \text{for} \quad \frac{R}{\lambda^{L-1}} < r < R . \tag{2}$$
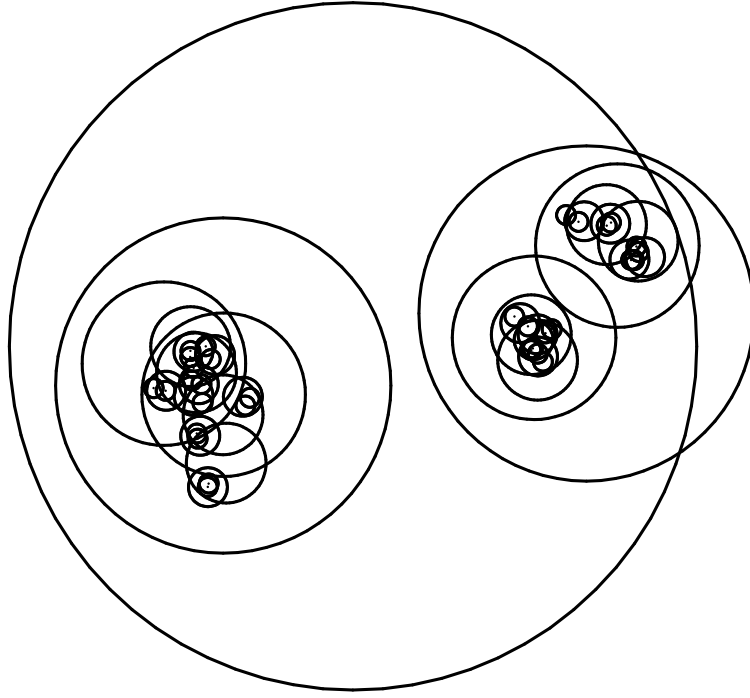
Fig. 1. The Soneira-Peebles model. Inside a level-0 sphere η level-1 circles are placed with a radius which is smaller by a fixed factor. This process is repeated until one ends up with η^L level-L circles. At the center of these level-L circles η^L points are placed, which form the resulting Soneira-Peebles point distribution.

The parameters η and λ may be chosen such that the two-point correlation function of the resulting point distribution matches the two-point correlation function of the observed galaxy distribution.

From Fig. 1 it may be appreciated that the Soneira-Peebles model involves a hierarchy of structures of varying densities and characteristic scales, with the higher level spheres corresponding to high-density structures of small scale and the lower level spheres corresponding to low-density structures of larger scale. As each of the spheres is constructed in the same way, the resulting point distribution is self-similar and forms a bounded fractal. The fractal geometry of a point set is often characterized by the fractal dimension D, which is defined as

$$D = \lim_{r \to 0} \frac{\log N(r)}{\log (1/r)} . \tag{3}$$

Here $N(r)$ is the number of non-empty cells in a partition of constant cell size r. If the Soneira-Peebles model would contain an infinite amount of levels, the resulting point
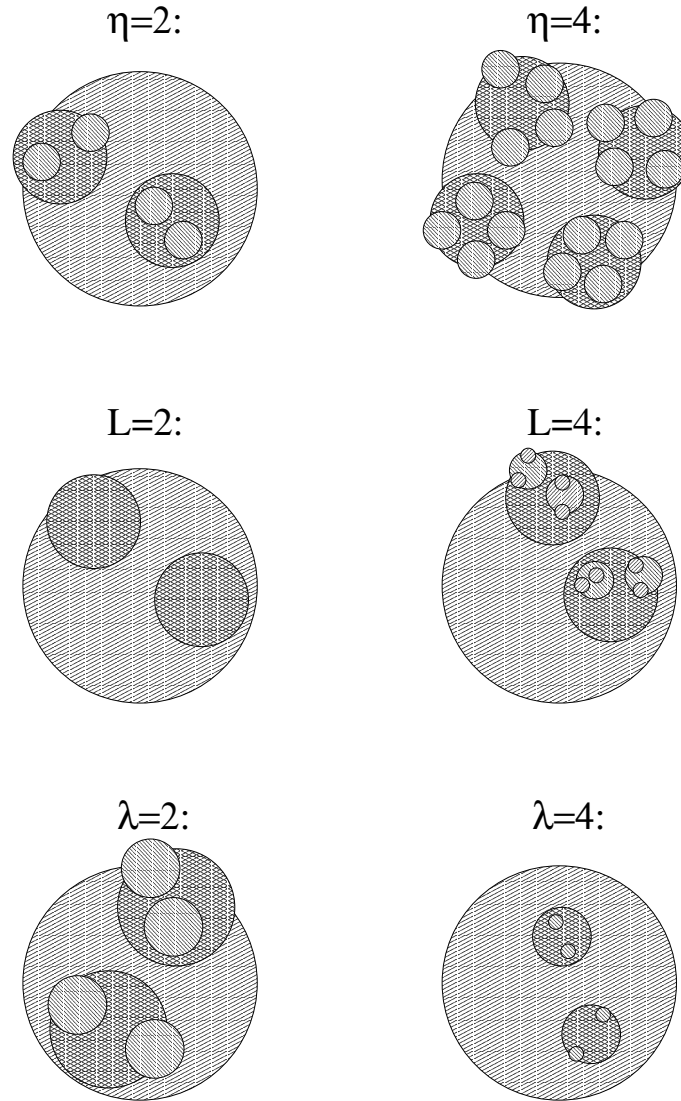
η=2:   η=4:

L=2:   L=4:

λ=2:   λ=4:

Fig. 2. The physical meaning of the three defining parameters η, L and λ of the Soneira-Peebles model. The upper row shows the effect of varying η, the number of circles which is placed in each circle. The central row shows the effect of varying L, the total number of levels. The bottom row shows the effect of varying λ, the ratio of the radius of each circle with the radius of subsequent circles of one level higher.

distribution would have fractal dimension $D = (\log \eta)/(\log \lambda)$ (we refer the reader to Martinez et al. (1990) for an extensive description of the fractal-like properties of the Soneira-Peebles model.

The original Soneira-Peebles model, which here we will refer to as the *extended Soneira-Peebles model*, consisted of the superposition of several singular Soneira-Peebles models with different values for η, λ and L. The ranges of values used for η, λ and L were chosen such that the resulting point distribution resembled the galaxy distribution in the Lick survey and simultaneously the observed two- and three-point correlation functions. Subsequently, absolute magnitudes were assigned to the points according to a particular luminosity distribution such that the apparent magnitude distribution of the projected point distribution resembled that of the projected apparent magnitude distribution of the galaxies in the Lick survey.

Table 1. Overview of a number of relevant properties of the $\eta = 2$ and $\eta = 4$ singular Soneira-Peebles model realizations. R_L denotes the radius of the level-L circles. The filling factor is the fraction of space occupied by the level-L circles. $\langle d \rangle$ denotes the mean distance between nearest neighbors. The peak density is defined as the inverse of the area of the level-L circles.

	realization 1	realization 2
η	4	2
λ	1.90	1.75
L	8	14
#points	65 536	16 384
R_L	$2.9 \cdot 10^{-3}$	$2.0 \cdot 10^{-4}$
filling factor	0.41	$1.6 \cdot 10^{-3}$
$\langle d \rangle$	$1.2 \cdot 10^{-3}$	$2.5 \cdot 10^{-4}$
peak density	$3.7 \cdot 10^{5}$	$8.1 \cdot 10^{7}$
fractal dimension D	2.2	1.2

1.1 Realizations: Singular Soneira-Peebles model

A number of different singular Soneira-Peebles model point distributions in two dimensions ($M = 2$) were constructed. As an illustration we describe two particular realizations. Realizations SPS1 is characterized by the parameter set $\eta = 4$, $\lambda = 1.9$ and $L = 8$. The total realization contains 65 536 points. The second set, SPS2, is specified by the parameters $\eta = 2$, $\lambda = 1.75$ and $L = 14$, yielding a distribution of in total 16 384 points. In both realizations the points have been placed in a box with periodic boundary conditions. The radius of the initial circle, in units of boxsize, is $R = 0.5$. In Table 1 we have listed some relevant quantities of these two realizations.

The resulting point distributions are shown in the top left-hand frames of Fig. 3 and 4. The subsequent frames in the top row zoom in on a particular smaller scale structure in the point distribution. The figures clearly show the differences between the realizations SPS1 and SPS2. The two models have a very different visual appearance. This can be mainly understood in terms of their different filling factors, the fraction of space occupied by the highest level circles. For the SPS1 $\eta = 4$ model this is more than two orders of magnitude larger than that of the SPS2 $\eta = 2$ model (see Table 1).

The two realizations also have a very different fractal dimension, $D = 2.2$ for the SPS1 $\eta = 4$ model and $D = 1.2$ for the SPS2 $\eta = 2$ model. It is indicative of the more extreme fractal distribution represented by the latter. Even the this distribution contains only a fourth of the number of points in the $\eta = 4$ SPS1 realization (see Table 1) it contains structures of a much larger dynamic range, both in density and in size, than the SPS1 model. The highest level circle has radius $R_L = 2.0 \cdot 10^{-4}$, resulting in a peak density (defined as the inverse area of this circle) of $8.1 \cdot 10^7$ points per volume unit, more than two orders of magnitude larger than in the $\eta = 4$ model. As an example of this in the third column we zoom in on a patch in the SPS2 $\eta = 2$ model with many more points than the equivalent region in the SPS $\eta = 4$ model (1024 vs. 297). It is a result of the clustering of points in such a way that prominent structures and features can be discerned over a larger range of scales and levels. The contrast in the spatial point distribution of the SPS1 $\eta = 4$ realization is clearly of a considerably lower level. On the other hand, the spatial distribution of the latter is characterized by a larger range in scale from level to level due to the higher value of λ.

1.2 Realizations: Extended Soneira-Peebles model

In the extended Soneira-Peebles model several singular Soneira-Peebles model point distributions are superposed on top of each other. Soneira & Peebles (1978) have shown that for certain choices of the parameters η, λ and L for the composing singular Soneira-Peebles models both the angular galaxy distribution as observed in the Lick survey and the observed angular two- and three-point correlation functions may be reproduced.

Superposing various different singular Soneira-Peebles realizations, each with a different self-similar behavior and dynamic range, produces a highly complex spatial point distribution containing structures and features over a large range of scales and with highly varying densities. We have constructed a point distribution SPE1 following this recipe. We have added 30 singular Soneira-Peebles realizations with $\eta = 2$ and $\lambda = 1.75$ and with L varying between 7 and 16. The resulting point distribution consists of 111 936 points and is shown in the top left frame of Fig. 5.
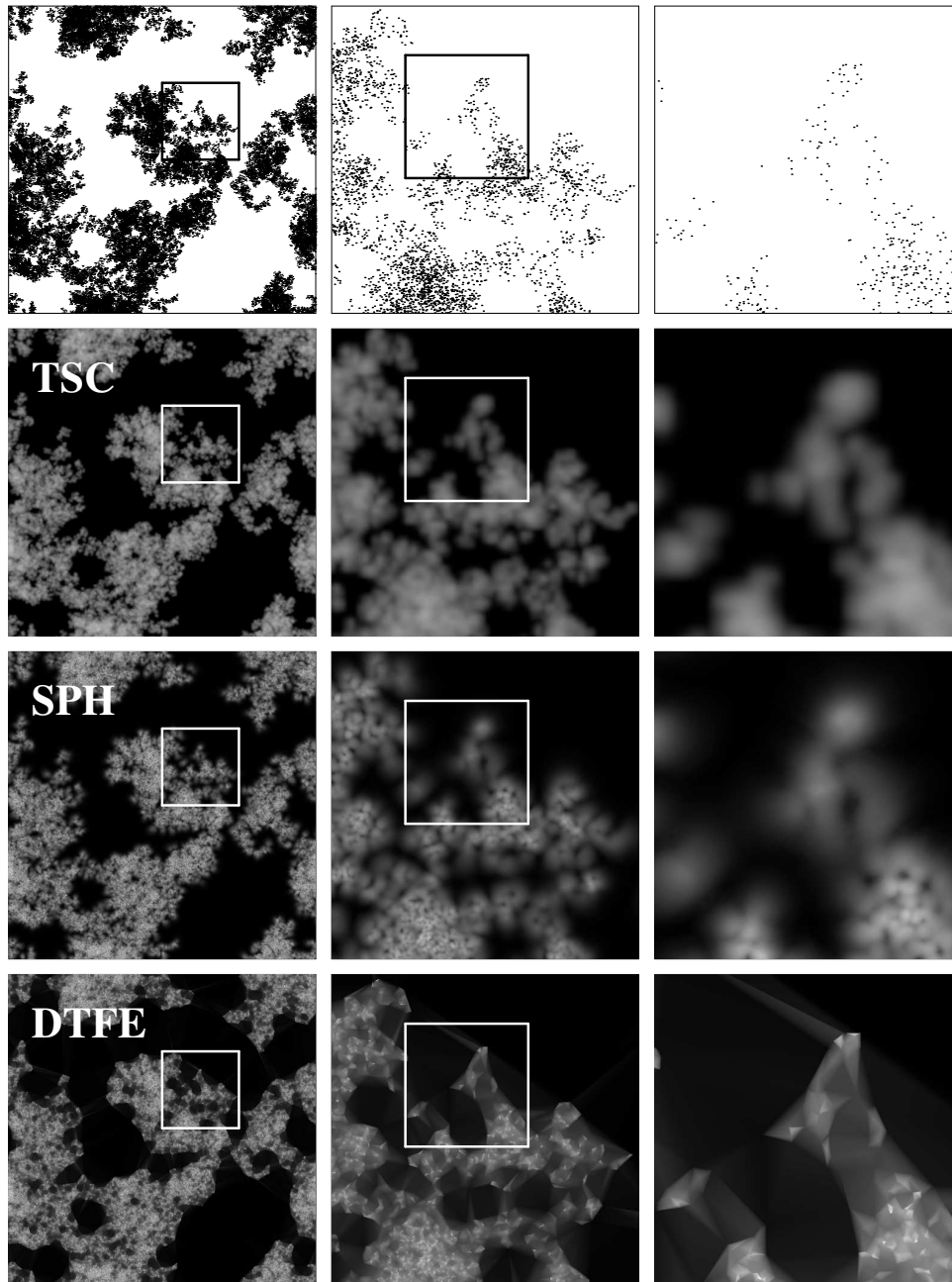
Fig. 3. Singular Soneira-Peebles model with with $\eta = 4$, $\lambda = 1.9$ and $L = 8$. Top row: full point distribution (left-hand frame) and zoom-ins focusing on a particular structure (central and right-hand frames). Rows 2 to 4: corresponding density field reconstructions produced using the TSC, SPH and DTFE methods.
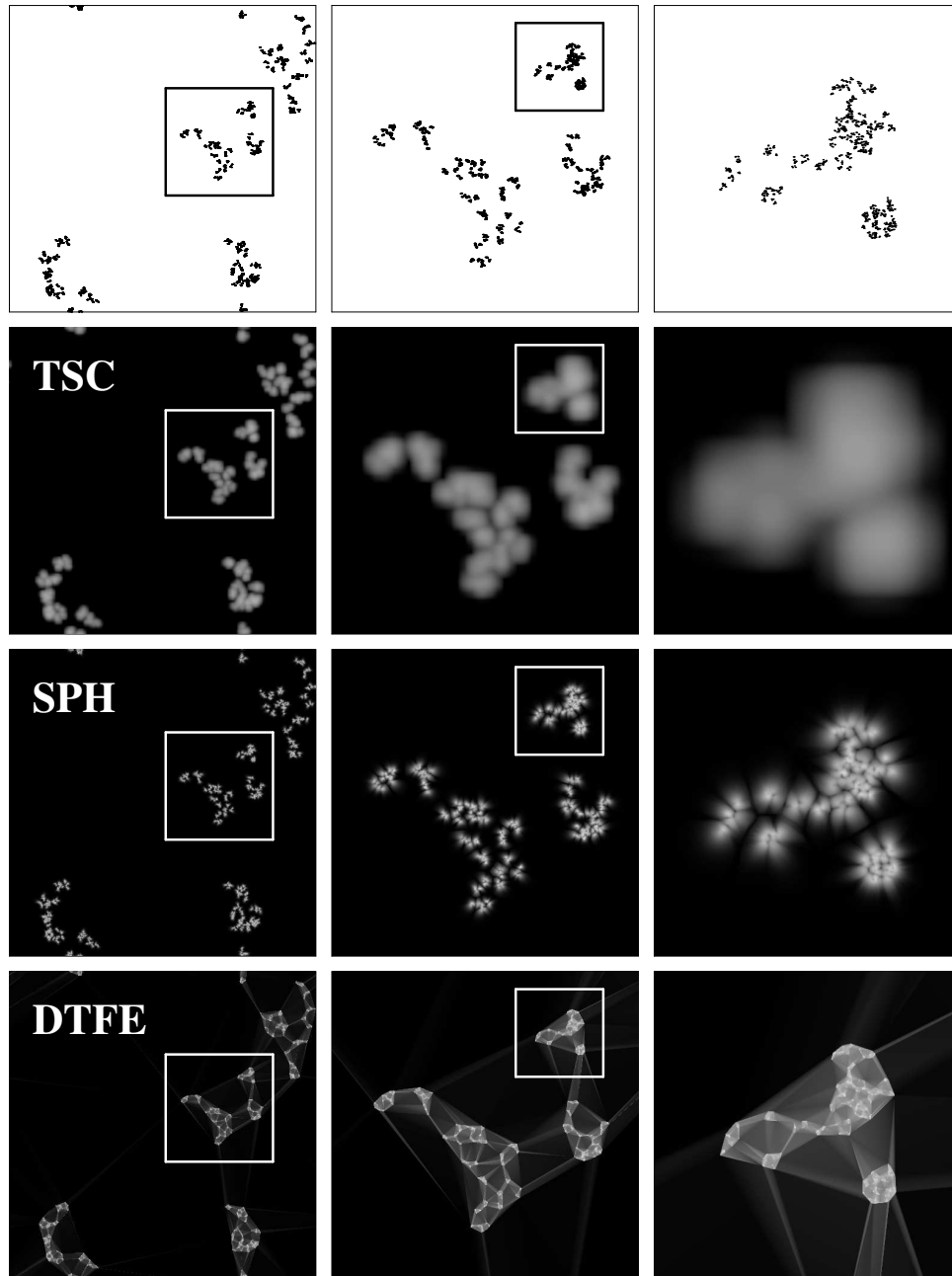
Fig. 4. Singular Soneira-Peebles model with $\eta = 2$, $\lambda = 1.75$ and $L = 14$. Top row: full point distribution (left-hand frame) and zoom-ins focusing on a particular structure (central and right-hand frames). Rows 2 to 4: corresponding density field reconstructions produced using the TSC, SPH and DTFE methods.
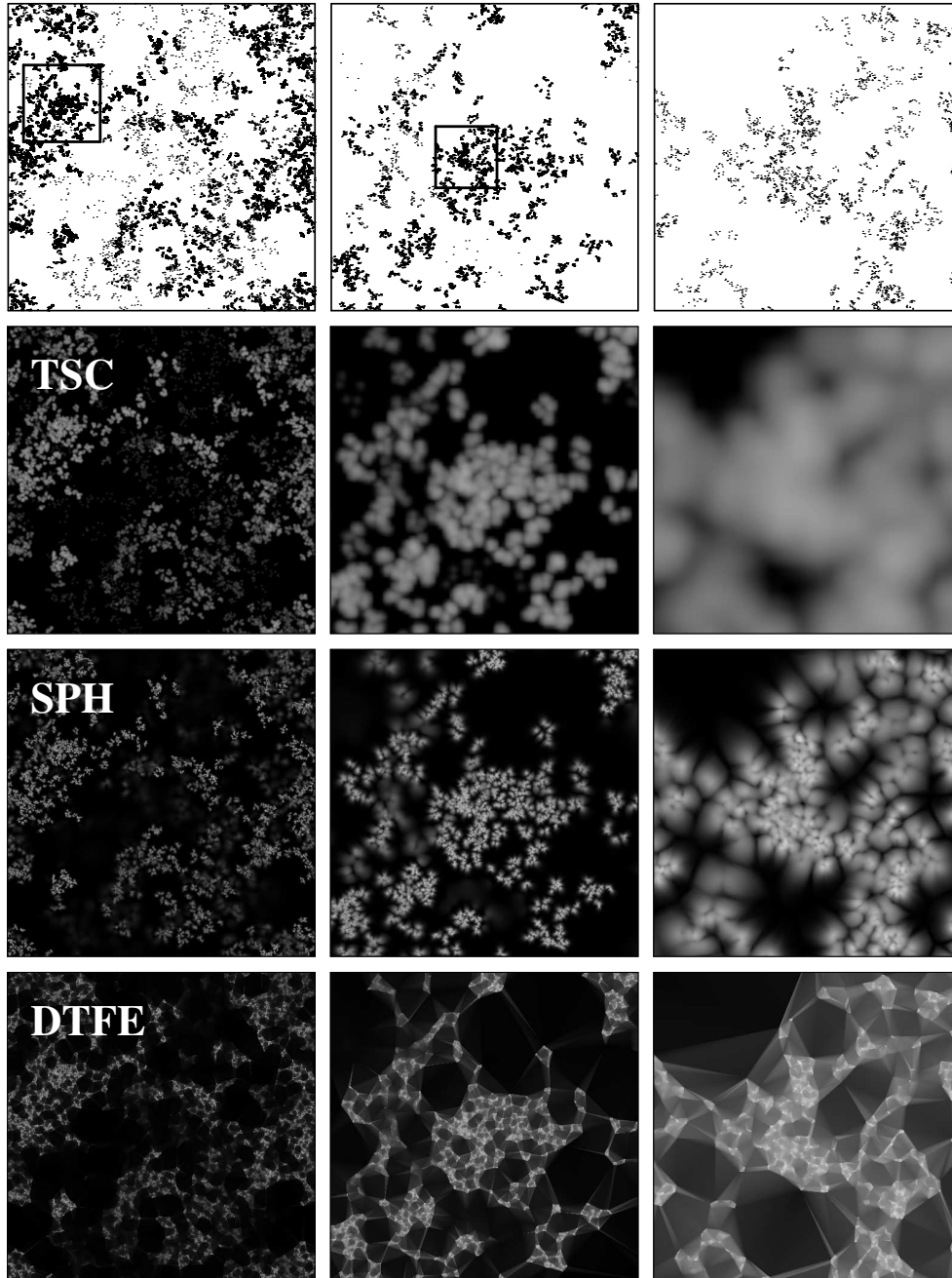
Fig. 5. Extended Soneira-Peebles model. Top row: full point distribution (left-hand frame) and zoom-ins focusing on a feature with interesting substructure (central and right-hand frame). Rows 2 to 4: corresponding density field reconstructions produced using the TSC, SPH and DTFE methods.

2 Density Field Reconstructions

We have reconstructed the density fields which correspond to the $\eta = 4$, $\eta = 2$ and extended model point distribution realizations shown in the top column of Fig. 3, Fig. 4 and Fig. 5 by means of a fixed, grid-based TSC reconstruction procedure, an adaptive SPH-like reconstruction prescription and the DTFE procedure. Gray-scale images of the corresponding density field reconstructions are shown in Fig. 3, Fig. 4 and Fig. 5: the 2nd column depicts the TSC density field reconstruction, the third column the SPH density field reconstruction and the 4th column the DTFE field reconstruction. In each case the lefthand column corresponds to the density distribution in the full box, while the next two columns depict the density field in successive zoom-ins. These have been selected according to whether they contain interesting features.

2.1 The $\eta = 4$ singular model

First consider the less extreme case of the $\eta = 4$ SPS1 model, shown in Fig. 3. The highest level circle has radius $R_L = 2.9 \cdot 10^{-3}$, resulting in a peak density (defined as the inverse area of this circle) of $3.7 \cdot 10^5$ points per volume unit, more than two orders of magnitude lower than in the $\eta = 2$ SPS2 model. When inspecting the complete box (left-hand column) the reconstructions of the different methods appear to be qualitatively similar. The TSC reconstruction seems somewhat more blurry than the SPH and DTFE reconstructions: the TSC density field shows less contrast between low and high density structures. Also, structures appear to be somewhat more extended. On this scale the difference between the SPH and DTFE reconstructions is very small. The only noticeable difference is that the DTFE reconstruction have a somewhat crispier.appearance.

The differences between the various methods become more apparent when zooming in on particular patches in the density field reconstructions, as can be clearly appreciated from the central and righthand columns of Fig. 3. Going from TSC to SPH to DTFE structures are better resolved and are characterized by a higher contrast. Structures in the TSC density field reconstructions are more blurry than their counterparts in the SPH reconstructions, while the latter again are somewhat blurrier than the corresponding features in the DTFE reconstructions.

These differences in visual appearance can be directly related to the effective smoothing kernels corresponding to the reconstruction methods. The TSC procedure is based upon the use of a fixed and rigid grid. The method is therefore unable to trace local variations in the number density of the point distribution on scales smaller than the grid scale. This means that structures smaller than the size of a grid cell are unresolved and smeared out over the extent of at least one grid cell. The SPH kernel adjusts itself to variations in the sampling density, with a kernel size defined such that it always constains a certain amount of sample points. This number is usually in the range of a few dozen points. However, the SPH kernel is less sensitive to the configuration of the local point distribution than the DTFE kernel. Its shape is user-defined and fixed, in most cases spherical, and do not adjust to the local

point distribution. As a result the SPH kernels perform less than optimal when it encounters typical anisotropic features or sharp transition regions between distinct morphological features. The effective DTFE kernel not only adjusts itself to the local number density of sample points, with on average the least number of neighbour points, but also to the local variations in the geometry of the point distributions: it manages to trace elongated filamentary features, flattened features, large low-density regions or extremely compact high-density features automatically and without the need to specify a priori their shape.

In all reconstructions artefacts related to the characteristic geometry of the effective smoothing kernels are visible. In the case of the TSC procedure the rigid geometry of the TSC grid produces maxima which lie at the centers of grid cells. The SPH kernel, on the other hand, produces artefacts at the transition regions between different structures as it tends to preferentially sample from only one of the surrounding structures, usually the densest one, and subsequently interpolates according to the user-defined kernel shape instead of one defined by the local geometry. As a result it produces artificial wings which fall off smoothly towards the background, rendering a correction for the artificial wings very difficult. Also the DTFE reconstructions contain artificial wings at the outskirts of structures. These wings have a distinct triangular shape. They are particularly prominent at sites where the density drops very quickly to (almost) zero, yielding Delaunay triangles which suddenly become very extended. While these artificial wings are usually much more extended than the ones in the SPH reconstructions, be it that the corresponding density levels have a much lower amplitude than the SPH reconstructions. It is therefore much easier for DTFE to separate the wings from genuine structures.

2.2 The $\eta = 2$ singular model

Fig. 4 presents the resulting density reconstructions for the more extreme point distribution of the $\eta = 2$ singular Soneira-Peebles model SPS2. The reconstructions all clearly reveal the density and size characteristics of the $\eta = 2$ SPS2 model. The differences between the different reconstructions are more pronounced than in the case of the $\eta = 4$ SPS1 reconstructions. Evidently, the TSC method is incapable of reproducing the small scale structures in the density field. This is particularly evident from the righthand panel of Fig. 4. This finest zoom-in onto the $\eta = 2$ conglomerate contains a large number of points distributed over a range of substructures. TSC produces three featureless clouds over which the corresponding sampling points have been distributed. The three clouds occupy a much larger area than that of the original point clouds. More interesting are the differences between the SPH and DTFE reconstructions. Their typical artefacts are clearly visible in the depicted frames in the second and third row of Fig. 4. In the SPH reconstruction groups in the point distribution smear out gently into their surroundings, clearly showing the imprint of the (artificial) spherical filter. The DTFE reconstruction, on the other hand, can be seen to connect distinct groups of points with artificial low-level wings. This is a result of its inability to deal with regions of zero density. Of particular relevance is the comparison between the SPH and DTFE reconstructions in the finest zoom-ins (righthand

column). The DTFE reconstruction is considerably more successful in reproducing the substructure present in the point distribution. Unlike the SPH reconstruction it manages to detect the small sub-clumps in the point distribution.

2.3 The extended Soneira-Peebles model

A visual comparison of the different reconstructed density fields shown in Fig. 5 SPE1 provides the same impressions as that obtained from the figures of singular Soneira-Peebles models in figs 3 and 4. A major difference is that the extended Soneira Peebles model has a much more pronounced appearance than the singular Soneira Peebles models. This holds true for all three methods, the TSC, SPH and DTFE density field reconstructions.

While the SPH and DTFE density field reconstructions on the scale of the complete box (lefthand column), do appear to be relatively small we can already discern the more blurry nature of the TSC reconstruction. This impression is confirmed as we zoom in on the patch in the lefthand corner (central column of panels). The TSC procedure is unable to accurately describe the point distribution at scales smaller than the grid size. The rich and complex structures present in the point distribution on this scale have been smeared out into featureless blobs. The differences between the SPH and DTFE reconstruction also start to become apparent. In the DTFE reconstruction the artificial low-level wings connecting the different structures begin to show up, while in the SPH reconstructions the smooth and broad wings at the outside of structures start to become visible. In the finest zoom (righthand panels) the differences between the reconstruction methods start to dominate the appearance of the images. The SPH method smears out the point distribution into circular blobs with no internal distribution. The larger features get smeared out into their surrounding environment as is most apparent through the artificial wings which smoothly fall off into the background. The DTFE method does manage to recover all structures visible in the point distribution. At this level, however, also the artificial low-density wings become quite prominent and form clearly visible bridges between the main structures.

Although a visual comparison between the different reconstructions shows that there are strong differences between the reconstruction procedures, it is not obvious which reconstruction is the best representation of the Soneira-Peebles point distribution. What is clear that TSC does not provide a good representation as it fails to resolve small-scale structures. The differences between SPH and DTFE are more subtle and a more quantitative measure is needed to assess the performance of the different reconstruction procedures.